Adsorption and UV-Laserdesorption of NO/O/Ni(100)

Th.Mull, H.Kuhlenbeck, G.Odörfer, R.Jaeger, C.Xu, B.Baumeister, M.Menges, G.Illing, and H.-J.Freund

Physikalische Chemie 1, Ruhr-Universität Bochum, D-4630 Bochum, FRG

D.Weide, and P.Andresen

Max-Planck-Institut für Strömungsforschung, D-3400 Göttingen, FRG

1. Abstract

We have studied adsorption as well as thermal and UV-laser (193 nm) desorption of NO adsorbed on Ni(100), on O(c2x2)/Ni(100) and on epitaxially grown oxides NiO(111) and NiO(100) using HREELS, XPS, NEXAFS, LEED and TPD. We find NO on NiO to be weakly chemisorbed. Laser desorption is only induced from the oxidic surfaces. Laser desorption cross sections are two orders of magnitude higher than gas phase photoabsorption cross sections for NO.

NO_2/NiO(100) has been studied via XPS, LEED and TPD. NO is probably the predominant desorption product under UV laser impact /1/. Reaction takes also place under XPS influence and under impact of secondary electrons from the X-ray gun.

Possible desorption processes are discussed.

2. Introduction

Recently, the photochemistry of small molecules on metal oxide surfaces has received some attention /2-5/. Briefly, a study of the dynamics of the desorbing molecules reveals non-thermal features such as bimodal velocity distributions and spin dependent rotational state populations, i.e. an underpopulation of the $^2\pi_{3/2}$ state by a factor of 40 as compared to the $^2\pi_{1/2}$ state for low rotational quanta.

Here we present new data concerning the NO desorption yields from different systems and discuss possible desorption mechanisms in light of a better chemically and structurally characterized oxide surface.

3. Experimental

A standard UHV System was used containing facilities for LEED, AES, XPS and TPD. The sample could be cooled down to 90 K by a liquid nitrogen reservoir and heated radiatively up to sufficient high temperatures. The Ni-crystal was cleaned by argon ion bombardment and repeated redox cycles as described in the literature (e.g./6/). NiO(111) was prepared by exposure of Ni(100) to 500 L O_2 at room temperature (/7/). Repeated cycles of oxygen dosing (1000 L, $p=10^{-5}$mbar) at T=570 K and subsequent annealing to T=670K lead to pure NiO(100).

4. Results

4.1. NO adsorbed on clean and oxidized Ni(100)

We have investigated NO desorption from clean Ni(100), c(2x2)O/Ni(100) and epitaxially grown nickel oxides NiO(111) and NiO(100). We find measurable desorption of NO (as judged by N1s intensities) under UV laser irradiation only for the nickel oxides. See fig. 1. The highest desorption cross section is reached for NO/NiO(100) with $7x10^{-17}$ cm^2 /4/. This finding is compatible with EELS data and XPS N1s structures and energies /4/ showing that NO/NiO(100) is a weakly bound system.

It is known that the NO desorption from NiO(100) starts from only one adsorption site and that in this case the NO axis is probably tilted to the surface normal by about 45°. The desorption cross section is more than two orders of magnitude above the average NO gas phase photoabsorption cross section in the wavelenght region around 193 nm of $1.1x10^{-19}$ cm^2, /8/.

It was found that NO desorption takes place also under influence of the soft X-rays of the X-ray gun (Al K_α).

4.2. NO_2/NiO(100)

NO_2 is of interest because in NO_2 adsorbate systems NO is found to be the main desorption result under 193 nm laser irradiation (/1/), as well as under electron impact (/9/).

NO_2 adsorbs on NiO(100). TPD- and XPS-spectra show that there are several species on the surface, i.e. N_2O_4, growing in intensity with higher exposure and NO_2 already present at low coverage. Our binding energies are in excellent agreement with those reported by Fuggle and Menzel for the same molecular species on W(110) (/10/).

UV laser desorption with the NO_2 species - as judged by XPS N1s (see fig.2) and O1s intensities - takes place with cross sections from $3x10^{-19}$ cm^2 for the monomer species up to $4x10^{-18}$ cm^2 for the dimer species (see fig. 3). The monomer value has to be compered with the NO_2 gas phase photoabsorption cross section ($6x10^{-19}$ cm^2, as derived from /11/).

The system NO_2/NiO(100) is unstable under XPS influence, see fig. 4. This destruction may partially occur via the same - unknown - reaction channels as the laser desorption at a much lower photon energy. As far as the photon flux of the X-ray gun is not yet calibrated, the cross sections cannot be compared directly. Reaction of the dimer species is also caused by secondary electrons emitted from the Al-foil of the X-ray window. This can easily be seen by the influence of a bias of -30 V that was applied to the sample.

However we want to state that electron- and XPS influences are irrelevant for the cross sections shown in fig. 3, because every point is subject to the same alteration and the intensities are related to each other.

5. Discussion

Two observations indicate a non thermal cause for the desorption of NO molecules from NO/NiO (/2,3/) as well as from NO_2 adsorbates on metal surfaces (/1/):

One of them is the observation of bimodal velocity distributions. Both the low and high velocity-channels seem to be of non-thermal origin for both are not well-described by Maxwell velocity distributions, although this is particularly true for the fast channel.

The second point is a large difference in the populations of different spin states at low rotational quanta /3/. Such an underpopulation can be understood as a consequence of the desorption mechanism in different ways:

The desorption can be a direct process: According to quantum mechanical calculations of Corey et al. (/12/) a desorption process induced by a neutral-neutral transition could be described in terms of the second half of a scattering process. The populations of the final rotational states are dependent on the orientation of the unfilled π orbital of the NO molecule in the initial configuration. It can lie either in the plane spanned by the molecular axis and the surface normal (NO being tilted by approximately 45°) or perpendicular to this plane and is responsible for different potentials felt by the desorbing NO molecule. The calculated final state distributions for different potentials already show underpopulation of the $^2\pi_{3/2}$ state. But the strength of the experimentally observed effect is not described by such calculations quantitatively.

On the other hand the desorption could be an indirect process as well. For example, the photon creates an electron-hole pair or a free electron and the electron is transferred to the molecule. Consequently a negative ion is formed which may lead to desorption. Some evidence is found by Hasselbrink et al. (/1/) who report the desorption yield as a function of laser energy, the light polarization and angle of incidence to be incompatible with direct excitation.

Thinking about the spin effect one may have to consider the antiferromagnetic properties of NiO (/13/). But in how far the transfer of a spin polarized electron may be involved in the desorption process and thus lead to the strong spin effect cannot be decided at present.

Acknowledgements

We thank the Deutsche Forschungsgemeinschaft and the Ministerium für Wissenschaft und Forschung des Landes Nordrhein-Westfalen for financial support.

References

/1/ E. Hasselbrink, S. Jakubith, S. Nettesheim, M. Wolf, A. Cassuto and G. Ertl, to be published

/2/ F. Budde, A. V. Hamza, P. M. Ferm, G. Ertl, D. Weide, P. Andresen and H.-J. Freund Phys.Rev.Lett. 60 (1988) 1518; see also: F. Budde, Thesis, Technische Universität Berlin, 1988

/3/ P. M. Ferm, F. Budde, A. V. Hamza, S. Jakubith, G. Ertl, D. Weide, P. Andresen and H.-J. Freund, Surf.Sci. 218 (1989) 467

/4/ H. Kuhlenbeck, G. Odörfer, R. Jaeger, C. Xu, T. Mull, B. Baumeister, G. Illing, M. Menges, H.-J. Freund, D. Weide, P. Andresen, G. Watson, E. W. Plummer, Vacuum, Proceedings of the 11th International Vacuum Congress and 7th International Congress on Solid Surfaces, Cologne, FRG (1989), to be published

/5/ Th. Mull, M. Menges, B. Baumeister, G. Odörfer, H. Geisler, H. Kuhlenbeck, H.-J. Freund, D. Weide, U. Schüller, P. Andresen, F.Budde, P. M. Ferm, A. V. Hamza and G.Ertl., Phys.Scripta, to be published

/6/ B. E. Koel, D. E. Peebles, J. M. White, Surf.Sci. 125 (1983) 709

/7/ G. Dalmai-Imelik, J. C. Bertolini and J. Rousseau, Surf.Sci 63 (1977) 67

/8/ S. F. Marmo, J.Opt.Soc.Am. 43 (1953) 1186

/9/ A. R. Burns, D. R. Jennison and E. B. Stechel, Phys.Rev.B, to be published

/10/ C. Fuggle and D. Menzel, Surf.Sci. 79 (1979) 1

/11/ T. Nakayama, M. Y. Kitamura, K. Watanabe, J.Chem.Phys. 30 (1959) 1180
/12/ G. C. Corey, J. E. Smedley, M. H. Alexander, W.-K. Lin, Surf.Sci. 191 (1987) 203
/13/ C. Kittel, Einführung in die Festkörperphysik, Oldenbourg Verlag, München - Wien, 6th ed. (1983) 515.

Figure captions

Fig. 1, a) and b): Laser desorption of NO from the different surfaces

▼ NO/NiO(100)/Ni(100), $\sigma \approx 7 \times 10^{-17}$ cm^2
◆ NO/(NiO(111)/Ni(100), $\sigma \approx 1.4 \times 10^{-17}$ cm^2
○ NO/c(2x2)O/Ni(100)
□ NO/Ni(100)

Fig. 2): XPS spectra of 5 L NO_2/NiO(100) under laser impact

Fig. 3): Decrease of XPS intensities

▼ NO_2/NiO(100), N1s, $\sigma \approx 3 \times 10^{-19}$ cm^2
■ N_2O_4/NiO(100), N1s, $\sigma \approx 4 \times 10^{-18}$ cm^2 ... 7×10^{-19} cm^2
◆ N_2O_4/NiO(100), O1s, $\sigma \approx 4 \times 10^{-18}$ cm^2

Fig. 4): Influences of X-rays and electrons on the NO_2 adsorbate

▽ NO_2/NiO(100)/Ni(100), unbiased
▼ NO_2/NiO(100)/Ni(100), biased
□ N_2O_4/NiO(100)/Ni(100), unbiased
■ N_2O_4/NiO(100)/Ni(100), biased

Laser induced reaction

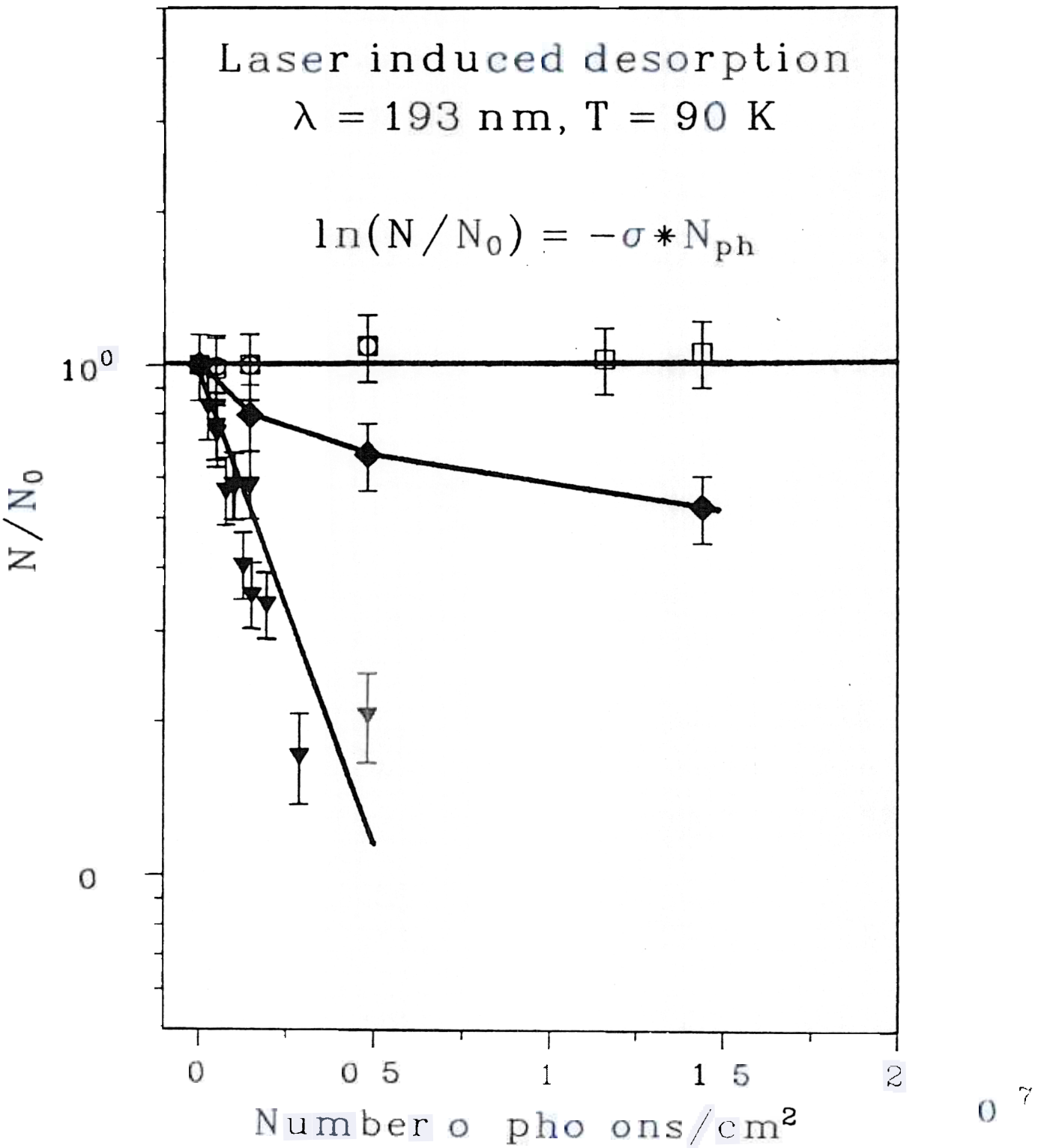

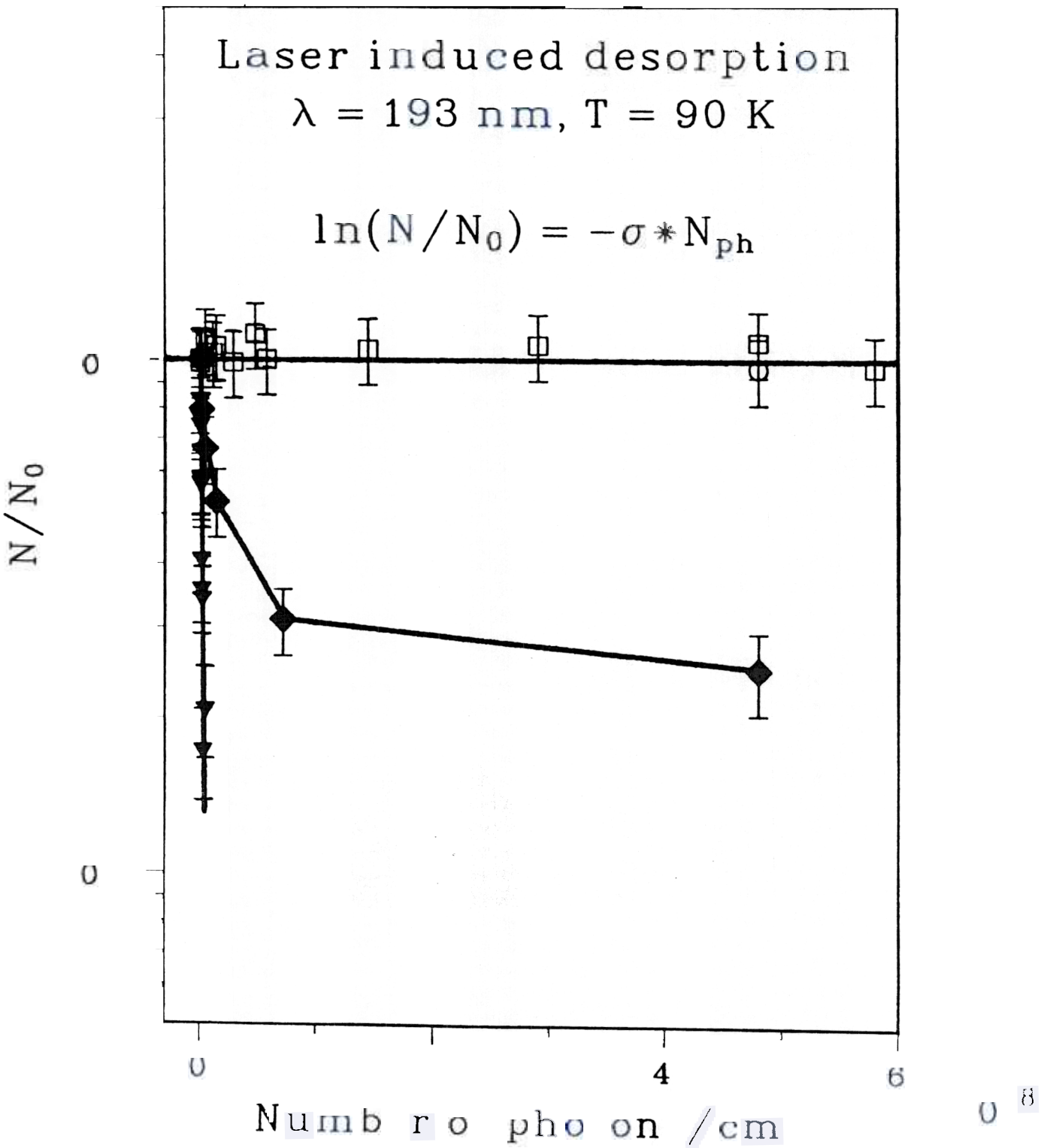
Laser induced desorption
λ = 193 nm, T = 90 K
ln(N/N0) = −σ*Nph
N/N0
0
0
0
4
6
Numb r o pho on /cm

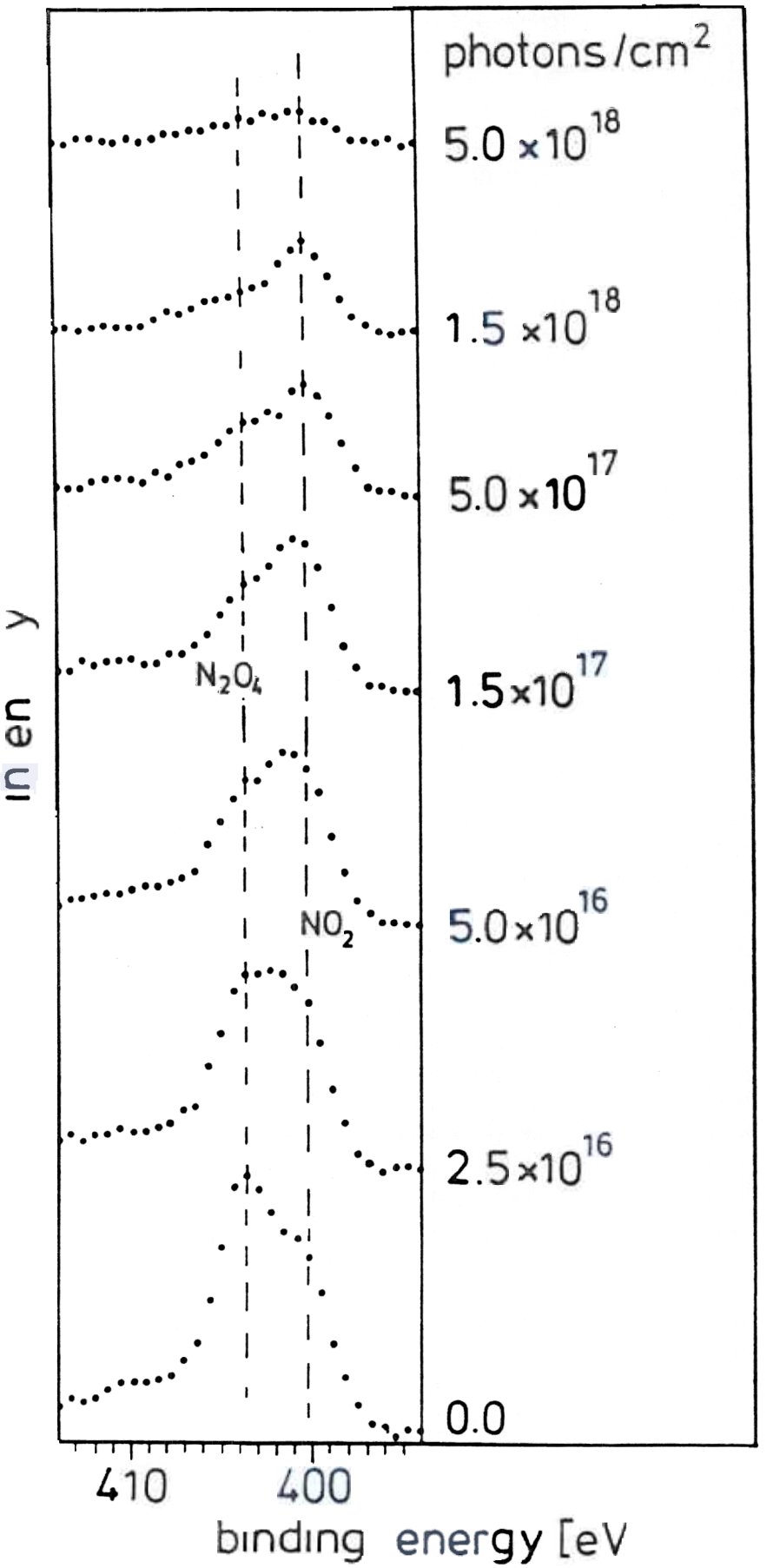
photons/cm²
5.0 ×10¹⁸
1.5 ×10¹⁸
5.0 ×10¹⁷
1.5×10¹⁷
5.0×10¹⁶
2.5×10¹⁶
0.0
N₂O₄
NO₂
410
400
binding energy [eV

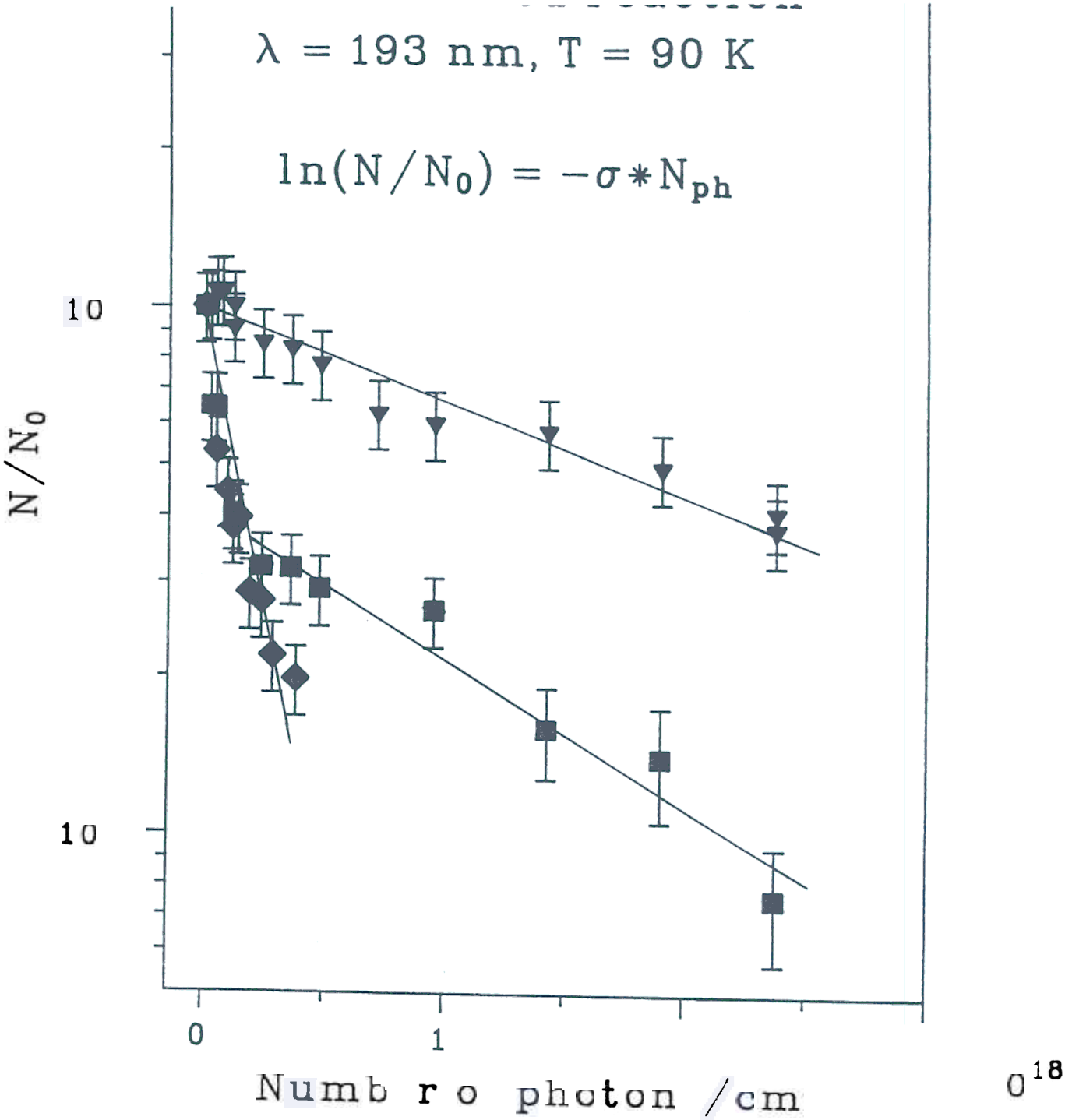
λ = 193 nm, T = 90 K
ln(N/N0) = −σ*Nph
N/N0
10
10
0
1
Numb r o photon /cm
0 18

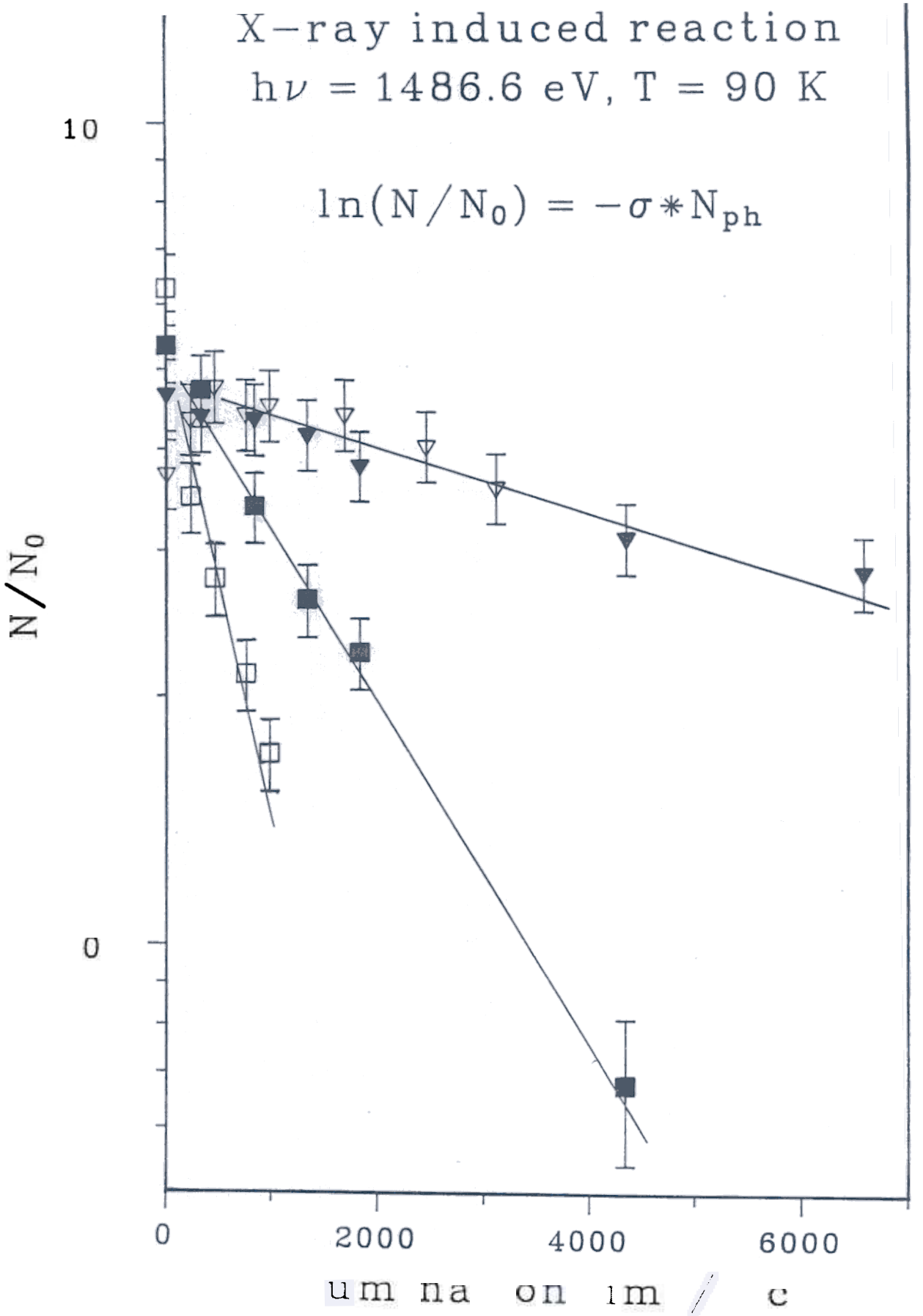
X-ray induced reaction
hν = 1486.6 eV, T = 90 K
ln(N/N0) = −σ*Nph
10
0
N/N0
0
2000
4000
6000
um na on im / c